How to Cite: Kukushkin, A.A., Kudashova, E.V., Root, E.V., Kositsyna, A.S., Ponomarev, I.S., Lyubyashkin, A.V., & Pustolaikina, I.A. (2025). Synthesis, Characterization and Computational Study of Novel Copper(II) Chelate Complexes Ligated by Pyridyl-Containing Beta-Diketonates. *Eurasian Journal of Chemistry, 30, 2(118), 4-18.* https://doi.org/10.31489/2959-0663/2-25-5

ORGANIC CHEMISTRY

Article

Received: 23 March 2024 | Revised: 30 April 2025 |
Accepted: 21 May 2025 | Published online: 28 May 2025

UDC 546.65; 547.442

https://doi.org/10.31489/2959-0663/2-25-5

Alexey A. Kukushkin[1*], Elizaveta V. Kudashova[2], Evgeny V. Root[2,3], Anna S. Kositsyna[1,2], Ilya S. Ponomarev[4], Alexey V. Lyubyashkin[2], Irina A. Pustolaikina[5]

[1]*School of Petroleum and Gas Engineering, Siberian Federal University, Krasnoyarsk, Russia;*
[2]*Siberian State University of Science and Technology named after Academician M.F. Reshetneva, Krasnoyarsk, Russia;*
[3]*Krasnoyarsk State Medical University named after Professor V.F. Voino-Yasenetsky University, Krasnoyarsk, Russia;*
[4]*Institute of Chemistry and Chemical Technology Siberian Branch of the Russian Academy of Sciences, Krasnoyarsk, Russia;*
[5]*Department of Physical and Analytical Chemistry, Karaganda Buketov University, Karaganda, Kazakhstan*
*(*Corresponding author's e-mail: alekseykukushkin@bk.ru)*

Synthesis, Characterization and Computational Study of Novel Copper(II) Chelate Complexes Ligated by Pyridyl-Containing Beta-Diketonates

Chelate complexes of copper(II) are widely used today in various sectors of the national economy, including medicine and pharmacology, biotechnology and agriculture, catalysis, and materials science. Pyridyl-containing β-diketones possess unique properties and can act as chelating ligands for metals, making them promising candidates for the development of metal-based pharmaceutical compounds. Therefore, the development and discovery of new copper(II) chelate complexes are of great interest and practical significance. In this work, new copper(II) chelate complexes of pyridyl-containing beta-diketonates were synthesized for the first time. Complexation between pyridyl-containing β-diketones and copper(II) acetate with molar ratio 2:1 was carried out in ethanol at a temperature not exceeding 50 ºC for 1 hour, with the yield of products ***IIIa–d*** ranging from 8.5 % to 31.3 %. The synthesized complexes were characterized using IR spectroscopy, atomic emission spectroscopy, and mass spectrometry, as well as DFT calculations, PASS prediction, and molecular docking. It was shown that all synthesized chelates exhibit biological activity as nicotinic receptor antagonists, with Pa values ranging from 0.821 to 0.915, and as dehydro-L-gulonate decarboxylase inhibitors, with Pa values exceeding 0.75. Molecular docking simulations with the alpha2 nicotinic acetylcholine receptor (PDB ID: 5FJV) confirmed high potential of synthesized chelates as nicotinic receptor antagonists and they can be recommended for further evaluation of therapeutic relevance through *in vitro* and *in vivo* studies.

Keywords: complexation, copper, diketone, atomic emission spectroscopy, mass spectrometry, IR spectroscopy, chelate, complex compound

Introduction

Copper chelate complexes are one of the most interesting classes of coordination compounds, since they are used as combustion catalysts for solid and liquid fuels, light stabilizers for various types of synthetic polymers [1], in the practice of gas chromatography [2]. Copper(II) chelate complexes are also known for their superoxide dismutase activity [3], as well as antibacterial, antifungal [4–6], anti-AchE [7], and antiproliferative effects against cancer cells [8]. It has been observed that interest in the synthesis and investigation of copper chelate complexes has grown significantly in recent years [9–12].

Copper is a crucial trace element involved in hematopoietic processes, the lack of copper exacerbates the lack of iron in iron deficiency anemia, causing additional depression of hemoglobin synthesis. Metal chelates are the most optimal form of a biogenic metal compound for the body. Thus, one study demonstrated the potential of a drug containing copper chelate complexes to stimulate hematopoiesis in animals [13].

Some copper triketone chelates such as diacetyl isovaleryl methane are used as fungicides and insecticides [1]. Also, the chelate form of copper demonstrates enhanced antimicrobial and wound-healing activity in therapeutic preparations compared to inorganic salts.

Chelate complexes of copper (II) showed anticancer activity [14]. Copper readily forms complexes with various bioactive organic ligands and serves as a convenient model for investigating ligand behavior with more expensive metals, such as platinum, palladium, etc. In turn, palladium(II) complexes can also exhibit biological activity [15]. There are a limited number of papers on the complexation of copper with pyridine-containing beta-diketones. Although such ligands are highly intriguing [16] and have potential applications in various fields [17, 18].

Therefore, the aim of this work was the synthesis of new copper chelate complexes of pyridyl-containing β-diketonates, their characterization and computational study using the *in silico* approach. Methods for *in silico* study of the physicochemical properties and potential biological activity of newly synthesized chemical compounds are now widely used due to the speed of implementation and relative low cost compared to *in vivo* and *in vitro* methods [19–21].

Experimental

Copper acetate II was obtained from LLC "JSC REACHIM" (Moscow, Russia). Ethyl alcohol was used as solvent [22].

IR spectra were recorded on an IR-microscope of "*SpecTRA TECH*" model "*InspectIR*" based on the IR-Fourier spectrophotometer "*Impact* 400" (USA). A sample of the substance was deposited onto a gilded plate, spread using a roller knife, positioned on a microscope stage, and analyzed using ATR spectroscopy. Analysis conditions included an MTC/A detector, a "*Si Caplugs*" lens, a wave number range of 400–650 cm^{-1}, a resolution of 1.928 cm^{-1}, 64 scans, and processing using OMNIC 5.1 E.S.P software.

Mass-spectra were recorded on a Shimadzu LC/MS-2020 device (Japan) with a RAPTOR ARC-18 100 column (2.1 mm diameter, 0.1 mm grain, 100 mm length) using a quadrupole Electron Injection Ion Source (ESI) mass spectrometer. The rate of direct injection of the sample and eluate composition was 10 µl/min. The scan range was 20–1000 Da.

The atomic emission spectrum was recorded on the ICAP 7400 instrument (USA).

Synthesis and Characterization

To study the reaction of the complexation of pyridyl-containing beta-diketones with copper, we synthesized β-diketones with pyridine substituents 1-phenyl-3-(pyridin-3-yl)propane-1,3-dion ***(Ia)***, 1-phenyl-3-(pyridin-4-yl)propane-1,3-dion ***(Ib)***, 1-(pyridin-3-yl)butane-1,3-dion ***(Ic)*** and 1-(pyridin-4-yl)butane-1,3-dion ***(Id)*** using the Claisen method, following a well-established procedure [23] (Figure 1).

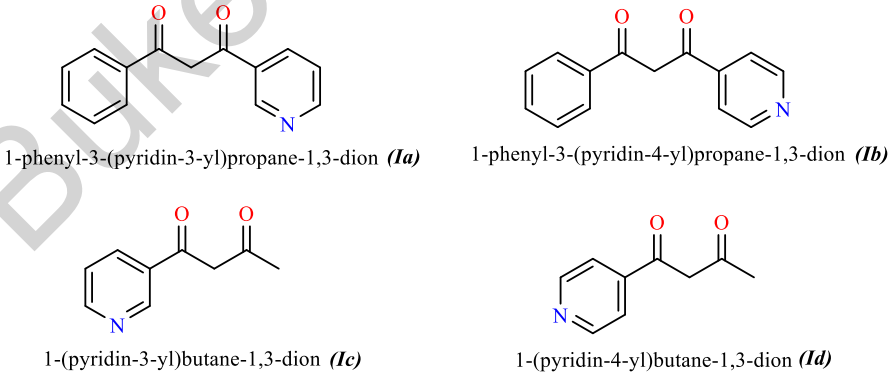

Figure 1 Synthesized pyridyl-containing beta-diketonates ***Ia-d***

The complexation of copper(II) acetate with synthesized pyridyl-containing beta-diketonates 1-phenyl-3-(pyridin-3-yl)propane-1,3-dion ***(a)***, 1-phenyl-3-(pyridin-4-yl)propane-1,3-dion ***(b)***, 1-(pyridin-3-yl)butane-1,3-dion ***(c)*** and 1-(pyridin-4-yl)butane-1,3-dion ***(d)*** was studied in various molar ratios of 1:1, 1:2, 2:1 (Table 1). The best results were obtained at a molar ratio of 2:1 [24].

Table 1

Chelate complexes yields at different molar ratio

Chelate complexes	R_1	R_2	Yield (%) at the 1,3- diketone : Cu(II) acetate molar ratio:		
			1:1	**1:2**	**2:1**
IIIa	Ph	β-Py	43	25	59
IIIb	Ph	γ-Py	55	27	61
IIIc	Me	β-Py	35	19	36
IIId	Me	γ-Py	40	25	43

We hypothesized that the formation of bis(acetylacetylacetonate) complexes was more likely, and the products obtained at a 2:1 ratio of 1,3-diketones to copper(II) acetate were selected as samples (Figure 2). The melting point was used as the comparison parameter. It was found that, for all studied ratios, both the melting point and the mixing sample analysis remained identical. Thus, all studied ratios yielded the same product, with the optimal formation conditions being a 2:1 ratio of 1,3-diketones to copper(II) acetate. Additional confirmation of the obtained samples' identity was achieved through thin-layer chromatography data.

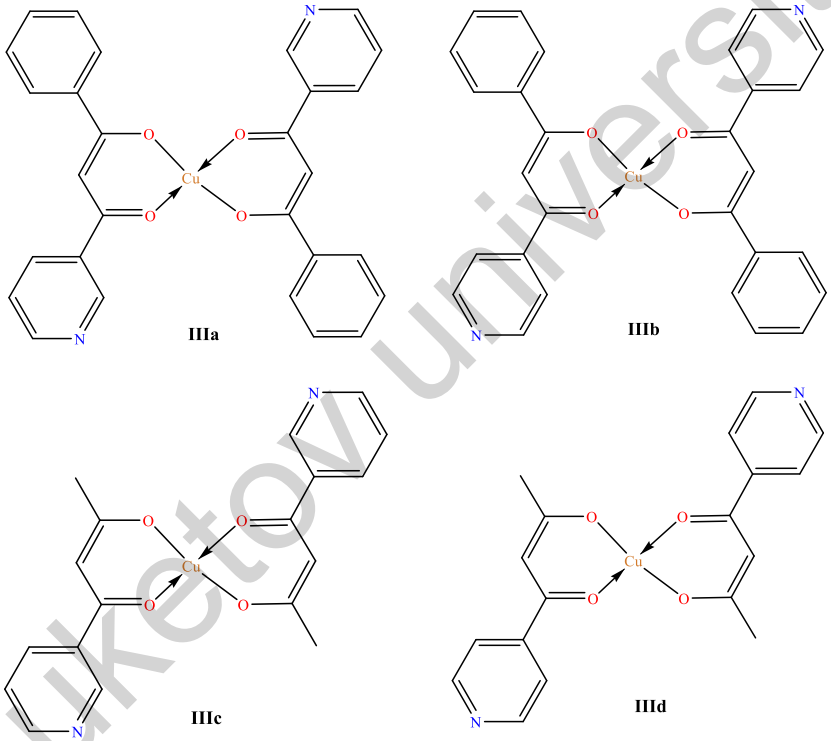

Figure 2. Structures of synthesized chelates ***IIIa-d***

Synthesis of Copper Chelate Complexes ***IIIa-d***

To 1,3-diketones ***Ia-d*** (0.004 mol), dissolved in a minimum amount of ethyl alcohol, copper acetate II (0.002 mol) in 70 % ethyl alcohol was added. The mixture was heated 1 hour at a temperature not higher than 50 ºC. The color of the solution changed from brown to green during the reaction. The green precipitate was filtered and air-dried. The purity of the resulting product ***IIIa-d*** was confirmed using thin-layer chromatography with a hexane-ethyl acetate eluent in a 5:1 ratio.

Bis(1-phenyl-3-(pyridin-3-yl)propane-1,3-dionate) Cu *(IIIa)*

Copper acetylacetonate with beta-pyridyl moiety and phenyl substituent *(IIIa)*. Yield 0.6 g (59 %), saturated green powder. IR spectrum, ν, cm^{-1}: 683, 887, 968, 1039, 1149, 1323, 1422, 1595, 1655, 1672, 3250. Mass spectrum, m/z (I, %): 511 (100) $[M]^+$, 513 (45), 512 (20). AES ICP (Cu) 8.5 %.

Bis(1-phenyl-3-(pyridin-4-yl)propane-1,3-dionate) Cu *(IIIb)*

Copper acetylacetonate with gama-pyridyl moiety and phenyl substituent *(IIIb)*. Yield 0.62 g (61 %), saturated green powder. IR spectrum, ν, cm^{-1}: 685, 747, 883, 966, 1038, 1149, 1329, 1425, 1597, 1687, 3076. Mass spectrum, m/z (I, %): 511 (100) $[M]^+$, 513 (45), 512 (20). AES ICP (Cu) 10.4 %.

Bis(1-(pyridin-3-yl)butane-1,3-dionate) Cu *(IIIc)*

Copper acetylacetonate with beta-pyridyl moiety and methyl substituent *(IIIc)*. Yield 0.28 g (36 %), light green powder. IR spectrum, ν, cm^{-1}: 691, 753, 1024, 1231, 1311, 1393, 1423, 1450, 1472, 1526, 1596, 3089. Mass spectrum, m/z (I, %): 387 (100) $[M]^+$, 389 (45), 988 (20). AES ICP (Cu) 22 %.

Bis(1-(pyridin-4-yl)butane-1,3-dionate) Cu *(IIId)*

Copper acetylacetonate with gama-pyridyl moiety and methyl substituent *(IIId)*. Yield 0.33 g (43 %), light green powder. IR spectrum, ν, cm^{-1}: 544, 643, 698, 725, 765, 1026, 1068, 1228, 1319, 1399, 1421, 1452, 1480, 1521, 1588, 1591, 3085. Mass spectrum, m/z (I, %): 387 (100) $[M]^+$, 389 (45), 988 (20). AES ICP (Cu) 31.3 %.

Computational Details

DFT Calculations

DFT calculations of copper chelate complexes ***IIIa-d*** were performed at the B3LYP/6-311++G(d, p) on organic (C, H, N, O, P) [25, 26] and LanL2DZ for metal (Cu(II)) [27] part basis set level of theory using Gaussian-16 [28]. In order to get as close as possible to the conditions of biological systems, solvation was taken into account in the calculations within the framework of the macroscopic polarizable continuum model CPCM (water) [29]. Optimization of the geometry of chelate complexes was carried out without any restrictions using the keywords OPT+FREQ; achieving geometry with a minimum of energy on the potential energy surface (PES) was confirmed by the absence of imaginary frequencies.

Based on the results of the DFT optimization of the geometry of the studied copper chelate complexes, HOMO-LUMO frontier orbitals and maps of the distribution of molecular electrostatic potential (MEP) were constructed and analyzed using analytical methods. The obtained values of the energies of the HOMO-LUMO orbitals were then used for calculations of such global descriptors of chemical activity [30], as: the ionization potential (IP), the electron affinity (EA), the energy gap ΔE_{gap}, molecular hardness (η) and softness (σ), the index of electrophilicity (ω) and nucleophilicity (ε), absolute electronegativity (χ) and chemical potential (μ):

$$IP = -E_{HOMO}, \quad (1) \qquad EA = -E_{LUMO}, \quad (2) \qquad E_{gap} = (E_{LUMO} - E_{HOMO}), \quad (3)$$

$$\chi = (IP + EA)/2, \quad (4) \qquad \mu = -(IP + EA)/2 = -\chi \quad (5) \qquad \eta = (IP - EA)/2, \quad (6)$$

$$\omega = \mu^2/2\eta, \quad (7) \qquad \sigma = 1/2\eta, \quad (8) \qquad \varepsilon = 1/\omega. \quad (6)$$

Visualization of DFT optimized molecular structures as well as frontier orbitals and MEPs were performed using GaussView 6.0 software [31].

In silico Study of Biological Activity

PASS (Prediction of Activity Spectra for Substances) program was used to predict useful biological activity of the synthesized copper complexes ***IIIa-d*** [32–34]. The PASS prediction, based on the molecular structure data, produces a list of probable activities, Pa being the probability of belonging to the "active" class, and Pi being the probability of belonging to the "inactive" class.

Molecular Docking Simulations

Molecular docking was performed using AutoDock Vina and AutoDock MGL Tools 1.5.7 [35, 36]. The molecular structure of the protein was downloaded from the Protein Data Bank (https://www.rcsb.org). Preparation of the protein molecular structure for docking included the steps of removing the native ligand and water molecules, protonation, and specifying the binding site. The position of the binding site was determined based on PDB data, and the following grid coordinates of the receptor active site were used: ($x = 12.881$, $y = 4.486$, $z = –0.184$) for the structure of alpha2 nicotinic acetylcholine receptor (PDB ID: **5FJV**). The docking results were used for comparative analysis of binding affinity and intermolecular interactions between the studied copper chelate complexes and the target protein. The study of intermolecular

interactions between the target protein and ligands was carried out using the BIOVIA Discovery Studio Visualizer 2017 [37] software.

Results and Discussion

We assumed that the resulting chelates have the structure ***IIIa-d*** (Scheme 1).

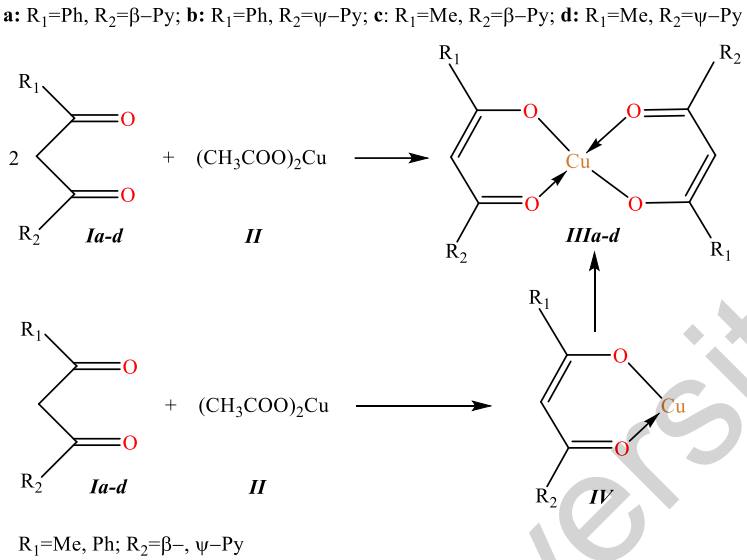

Scheme 1. Possible pathways for the copper chelates formation

The structure of the chelates was studied by IR spectroscopy. The IR spectra of chelates ***IIIa-d*** contain bands corresponding to phenyl and pyridyl fragments, observed in the range of 1680–1440 cm^{-1}.

At the same time, it is known that the ligands of copper acetylacetonate contain a conjugated bond system, –C(O)–CH=C–. The conjugation induces a bathochromic shift, manifesting as three bands at 1575, 1545, 1525 cm^{-1}, characteristic of a quasi-aromatic metallocycle [38]. In our opinion, for compounds ***IIIa-d***, the bands of stretching vibrations –C(O)–CH=C– at 1575, 1545, 1525 cm^{-1} are partially (for compounds ***IIIc***, ***IIId***) or completely (for compounds ***IIIa***, ***IIIb***) overlapped by stretching vibrations of the pyridine or phenyl fragments.

Indeed, the DFT Calculations performed for all chelates ***IIIa-d*** showed that with methyl and pyridyl substituents (compounds ***IIIc***, ***IIId***) the distortion of geometry at the Cu^{2+} ion is minimal. Whereas in the presence of pyridine and phenyl rings (compounds ***IIIa*** and ***IIIb***) there is a distortion of geometry in one of the ligands. A detailed description of the *DFT* Calculations results is provided in the Computational Study section of this article.

The next step in elucidating the structure of copper complexes was identifying the number of ligands. Although the reaction proceeded depending on the ratio of 1,3-diketone and copper(II) acetate, the formation of either structure ***III*** or ***IV*** remains possible (Scheme 1). To resolve the uncertainty regarding the formation of structure ***III*** or ***IV*** in the obtained chelate complexes, a chromato-mass spectrometric study was carried out.

The analysis revealed that the predominant compounds formed contained two molecules of a dicarbonyl compound per copper molecule, with molecular weights of 512 g/mol and 388 g/mol, respectively. Additionally, signals corresponding to compounds with one diketone molecule per copper molecule were observed, with molecular weights of 226 g/mol and 288 g/mol, as presented in Table 2.

Table 2

Results of gas chromatography-mass spectrometry analyses

Complex	R_1	R_2	Molecular weight, g/mol	Retention time, min	Peak area, %
IIIa	β-pyridyl	Ph	512	6.32	76.8
IIIb	γ-pyridyl	Ph	512	5.99	83.0
IIIc	β-pyridyl	Me	388	7.30	91.6
IIId	γ-pyridyl	Me	388	5.77	98.0

Additionally, sample analysis revealed that, over time, the content of chelates containing one diketone molecule per copper atom, with molecular weights of 226 g/mol and 288 g/mol, decreased. Simultaneously, the peak area of detectable compounds with molecular weights of 512 g/mol and 388 g/mol increased. This indirectly suggests the instability of product ***IV*** (Scheme 1) and the subsequent formation of product ***III*** (Scheme 1). Thus, we have demonstrated that chelates preferentially take form ***III***.

To confirm the amount of substance that reacted during synthesis, a study was conducted using atomic emission spectroscopy with inductively coupled plasma. The analysis determined the amount of copper that reacted with the original β-diketone. The results of the atomic emission analysis are presented in Table 3.

Table 3

Results of copper content analysis by the atomic emission spectroscopy

Complex	Me	R_1	R_2	Copper content, %
IIIa	Cu	β-pyridyl	Ph	8.5
IIIb	Cu	γ-pyridyl	Ph	10.4
IIIc	Cu	β-pyridyl	Me	22.0
IIId	Cu	γ-pyridyl	Me	31.3

In complex containing pyridine fragment and phenyl substituent amount of copper is 10.4 %, and in complex with methyl substituent and position of nitrogen in γ-position is 31.3 %. This is most likely due to the steric and electron donor properties of the substituents.

In the complex containing a pyridine fragment and a phenyl substituent, the copper content is 10.4 %. In contrast, the complex with a methyl substituent and nitrogen in the γ-position, contains 31.3 % copper. This difference is most likely attributed to the steric and electron-donating properties of the substituents.

Computational Study

DFT Calculations

Since chelate complexes of copper pyridyl-containing beta-diketonates were synthesized for the thirst time, it was interesting to study their physicochemical properties and biological activity using *in silico* methods. First of all, the geometry of the synthesized copper complexes ***IIIa-d*** was optimized by the DFT method with the use of the 6-311G++(d, p) and LANL2DZ basis sets for the ligands and its complexes, respectively, in conjunction with the B3LYP hybrid correlation functional taking into account solvation within the framework of the macroscopic solvation CPCM (water) model. Resulting geometry optimization 3D structures are shown in Figures 3 and **S1**.

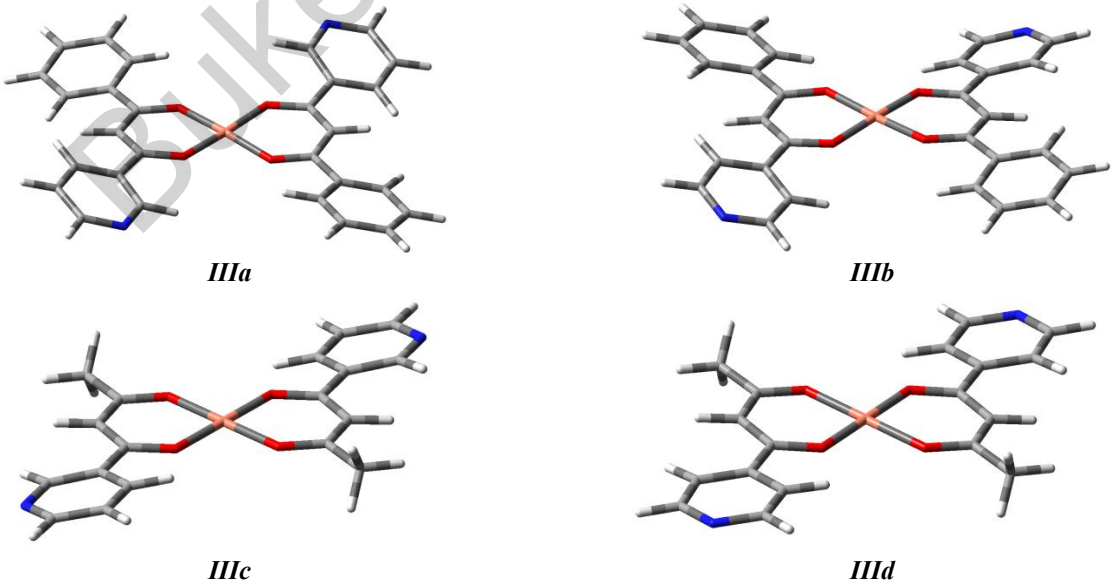

Figure 3 Optimized 3D structures of chelate complexes ***IIIa-d***

As can be seen in Figures 3 and S1, each copper atom forms a four-center bond with two bidentate diketone ligands in chelate complexes ***IIIa-d.*** In chelates ***IIIc*** and ***IIId,*** the central cyclic diketonate fragment with copper is almost planar, while the side pyridyl substituents have deviations from planarity of approximately 10° relative to the plane of the central fragment of the chelate. The structure of chelates ***IIIa*** and ***IIIb*** is more twisted due to the presence of 4 bulky side substituents, while the central cyclic diketonate fragment with copper has small deviations from planarity, while the side pyridyl substituents are rotated at a wider angle of about 17°, and the side benzene rings are rotated at an angle of about 13° relative to the plane of the central fragment of the chelate.

It should be noted that the structure of the resulting chelates is quite symmetrical, as a result of which compounds ***IIIa-d*** are characterized by small dipole moments of 0.2107, 0.1897, 0.0003 and 0.0004 Debye, respectively, which indicates a homogeneous charge distribution and a low level of polarity of the chelate complexes.

Frontier Molecular Orbitals and Molecular Electrostatic Potential Map (MEP) Analysis

Next, based on the optimized structures of synthesized copper complexes ***IIIa-d,*** the construction and analysis of the boundary HOMO-LUMO orbitals and Molecular Electrostatic Potential Map (MEPs) were performed (Figures 4, 5).

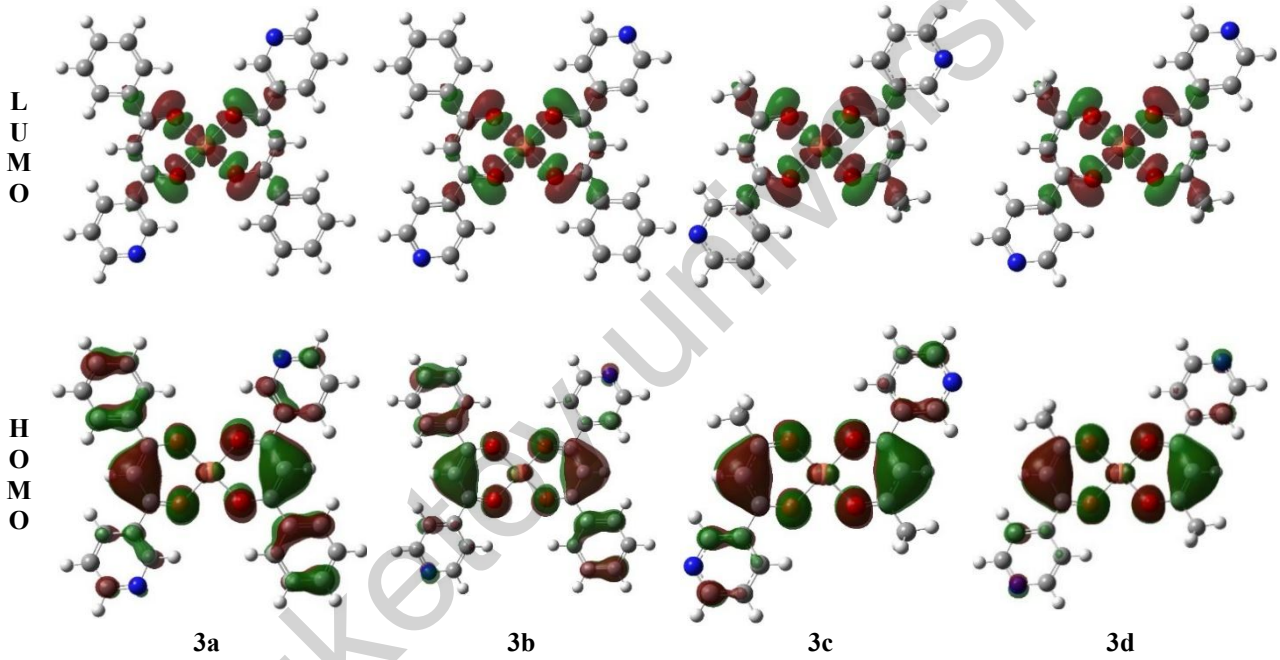

Figure 4. HOMO-LUMO orbital diagrams of chelate complexes ***IIIa-d***

As can be seen in Figure 4, the electron density on the HOMO and LUMO orbitals is localized in different places: LUMO is predominantly on the central cyclic diketonate copper containing fragment, while HOMO is more delocalized throughout the entire structure of the complex. Next, the location of electrophilic and nucleophilic centers in the studied complexes ***IIIa-d*** was assessed based on the analysis of the molecular electrostatic potential (MEP) (Figure 5).

As can be seen in Figure 5, the negative charge in the studied complexes ***IIIa-d*** is expectedly localized on the oxygens of the central cyclic diketonate fragment, as well as on the nitrogen heteroatoms; the positive charges are concentrated on the complex-forming metal atom, as well as on the hydrogen atoms of the cyclic diketonate fragment. Accordingly, this allows us to assume that the nucleophilic center of the studied copper complexes ***IIIa-d*** is localized on the oxygen and nitrogen atoms, whereas the electrophilic center can be correlated with the position of the complex-forming copper atom, as well as with the position of the hydrogen atoms of the cyclic diketonate fragment.

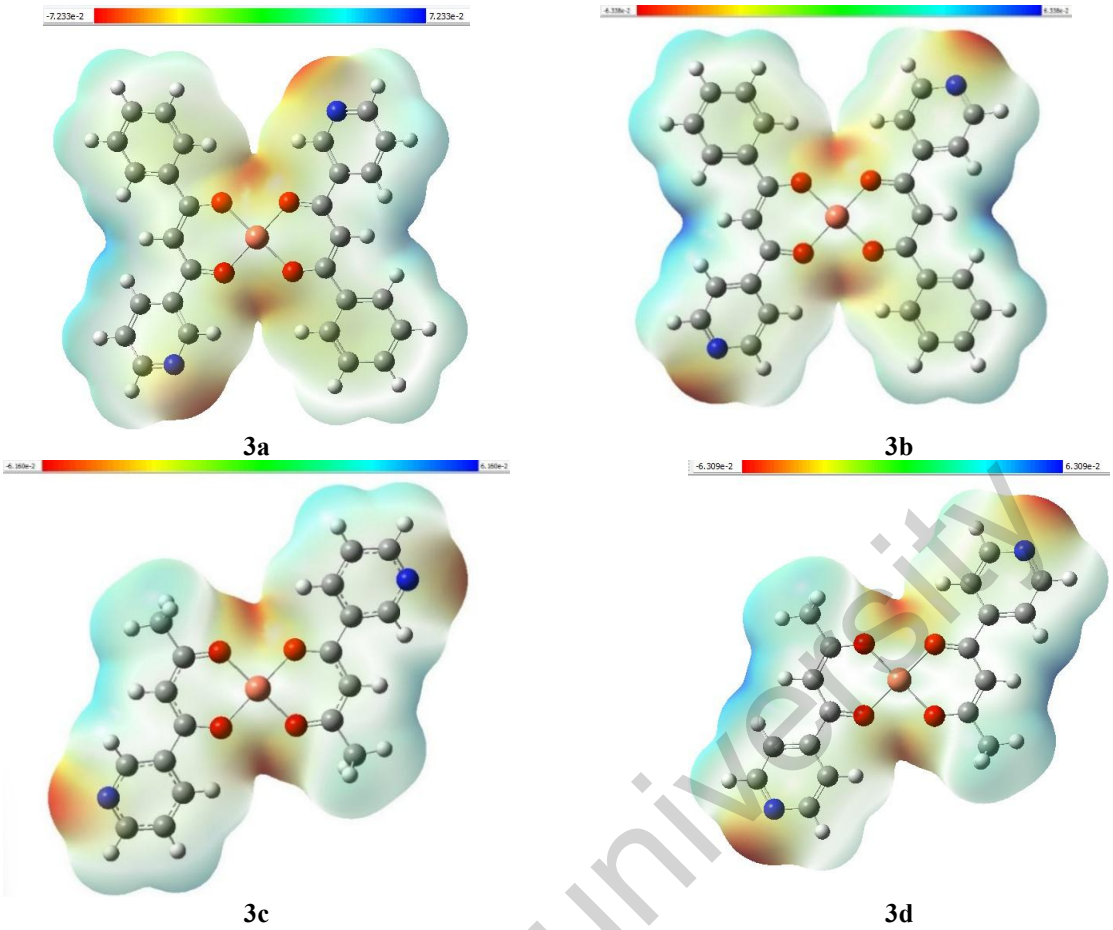

Figure 5 Molecular electrostatic potential map (MEP) of chelate complexes ***IIIa-d***

Global Reactivity Indexes

An assessment of the studied copper complexes ***IIIa-d*** global reactivity parameters was performed based on the calculated energy of HOMO-LUMO orbitals. The following global descriptors of chemical activity were assessed: ionization potential (IP), electron affinity (EA), energy gap ΔE_{gap}, molecular hardness (η) and softness (σ), chemical potential (μ), electrophilicity (ω) and nucleophilicity (ε) indexes, absolute electronegativity (χ) (Table 4).

Table 4

Global descriptors of chemical activity

Complex	IP, eV	EA, eV	ΔE_{gap}, eV	η, eV	σ, eV^{-1}	μ, eV	ω, eV	ε, eV^{-1}	χ, eV
IIIa	6.5652	3.2904	3.2748	1.6374	0.3053	–4.9278	7.4151	0.1348	4.9278
IIIb	6.6210	3.3344	3.2865	1.6432	0.3042	–4.9777	7.5392	0.1326	4.9777
IIIc	6.6409	3.2735	3.3674	1.6837	0.2969	–4.9572	7.2976	0.1370	4.9572
IIId	6.7106	3.3211	3.3894	1.6947	0.2950	–5.0158	7.4227	0.1347	5.0158

As can be seen in Table 4, the studied copper complexes ***IIIa-d*** are characterized by an electron affinity **EA** of about 3.2–3.3 eV and a fairly high ionization potential **IP** in the region of 6.5–6.7 eV, which indicates their low reducing properties. The energy gap ΔE_{gap} at the level of 3.2–3.3 eV indicates the chemical stability of the studied copper complexes ***IIIa–d***. The low value of molecular softness σ at the level of 0.3 eV^{-1}, together with the 1.6 eV value of molecular hardness indicates the hard nature of the studied complexes ***IIIa-d***. The negative value of the chemical potential μ and its value of (–4.9)–(–5.0) eV confirm the stability of the studied copper complexes. The high level of electrophilicity index ω in the range of 7.2–7.5 eV suggests a predominantly electrophilic nature of the reactivity of the studied complexes. The absolute electronegativity χ of the complexes ***IIIa-d*** lies in the range from 4.9 to 5.0 eV.

In silico Study of Biological Activity

Next, we used a PASS (Prediction of Activity Spectra for Substances) program to predict useful biological activity of the synthesized copper complexes ***IIIa-d***. This tool allows to estimate the probability of various types of biological activity for chemical compounds based on their structural formulas using such indicators as *Pa* — the probability of being active and *Pi* — the probability of being inactive. The predicted probabilities of biological activity are presented in the Table 5.

Table 5

PASS predicted biological activity potential of the complexes *IIIa-d*

*Pa**	*Pi**	**Type of activity**
IIIa		
0.887	0.004	Nicotinic receptor antagonist
0.783	0.011	Dehydro-L-gulonate decarboxylase inhibitor
0.753	0.001	Glutamylendopeptidase II inhibitor
IIIb		
0.890	0.004	Nicotinic receptor antagonist
0.811	0.010	Feruloylesterase inhibitor
0.787	0.011	Dehydro-L-gulonate decarboxylase inhibitor
IIIc		
0.867	0.005	Gluconate 2-dehydrogenase (acceptor) inhibitor
0.821	0.008	Nicotinic receptor antagonist
0.800	0.009	Dehydro-L-gulonate decarboxylase inhibitor
IIId		
0.915	0.003	Gluconate-2-dihydrogenase inhibitor (acceptor)
0.845	0.005	Nicotinic receptor antagonist
0.773	0.013	Dehydro-L-gulonate decarboxylase inhibitor
where: *Pa* — the probability of being active; *Pi* — the probability of being inactive.		

As can be seen in Table 5, all comlexes ***IIIa-d*** exhibited biological activity as nicotinic receptor antagonists with *Pa* values ranging from 0.821 to 0.915, and as dehydro-L-gulonate decarboxylase inhibitors, with *Pa* values above 0.75. Nicotinic receptor antagonists inhibit acetylcholine activity at nicotinic acetylcholine receptors (nAChRs) and are utilized in the treatment of hypertension, nicotine dependence, neurological disorders, and anesthesia. Gluconate-2-dehydrogenase inhibitor (acceptor) activity is strongly predicted for ***IIIc*** and ***IIId*** complexes, with high *Pa* values (0.867–0.915), suggesting a role in carbohydrate metabolism and in the treatment of type 2 diabetes and related cardiovascular diseases.

The analysis of the data presented in Table 5 indicates that complexes ***IIIa–d*** exhibited the highest biologically active potential as nicotinic receptor antagonists. This biologically active property of complexes ***IIIa–d*** is potentially very beneficial, as according to WHO data, more than 20 % of the world's population currently uses tobacco, with 8 million people dying each year from the consequences of tobacco use, including 1.3 million passive smokers. Therefore, the search for new nicotinic receptor antagonists is an important area of modern pharmacology, and we further study the inhibitory potential of complexes ***IIIa–d*** as nicotinic receptor antagonists using the molecular docking approach.

Molecular Docking Simulations

Nicotinic receptor antagonists bind with nicotinic acetylcholine receptors (nAChRs) [39]. These receptors are ion channels that perceive nicotine and acetylcholine, so their action is aimed at regulating the transmission of nerve impulses. Nicotinic acetylcholine receptors (nAChRs) are ligand-gated ion channels that, upon binding nicotine or acetylcholine, open, allowing sodium, potassium, and calcium ions to pass through the cell membrane. This results in depolarization of the cell and initiation of a signal important to the nervous system. nAChR antagonists block this process by preventing binding of nicotine or acetylcholine with the receptor. This results in the prevention of ion channel activation and, accordingly, the suppression of nerve signal transmission. This mechanism is used in pharmacology, for example, in drugs used to treat nicotine addiction or as muscle relaxants during surgery [40]. Target proteins for nicotinic acetylcholine receptor (nAChR) antagonists include receptor subtypes such as: α4β2 receptors are the most common nAChR

subtype in the central nervous system and have been linked to cognitive function and nicotine addiction.; α7 receptors — these receptors are involved in memory, learning and inflammatory processes, and are also a target for the treatment of neurodegenerative diseases [41].

According to the literature [42], alpha2 nicotinic acetylcholine receptor in pentameric assembly (PDB ID: **5FJV** [43]) may act as a target protein for nicotinic acetylcholine receptor antagonists (nAChR), so it was used for molecular docking simulations with synthesized copper complexes ***IIIa-d.*** Bupropion [44] and the native ligand [43] were used as reference drugs. Molecular docking simulation of the studied copper complexes ***IIIa-d*** with the target alpha2 nicotinic acetylcholine receptor (PDB ID:**5FJV**) was performed using the AutoDock Vina program; the obtained data on the binding affinity are presented in Table 6.

Table 6

Binding Affinity (kcal·mol⁻¹) of copper complexes *IIIa-d* with alpha2 nicotinic acetylcholine receptor (PDB ID: 5FJV)

Ligand	Binding Affinity, kcal·mol⁻¹
IIIa	–8.3
IIIb	–8.1
IIIc	–6.9
IIId	–6.6
Reference Drug	
Bupropion	–5.4
Native ligand (1S,2S,4R)-2-(6-chloropyridin-3-yl)-7-azabicyclo[2.2.1]heptane	–5.9

The data presented in Table 4 show that the studied copper complexes ***IIIa-d*** demonstrate higher binding affinity (–8.3, –8.1, –6.9 and –6.6 kcal·mol^{-1}, respectively) with the alpha2 nicotinic acetylcholine receptor (PDB ID:**5FJV**) compared to the reference drugs Bupropion (–5.4 kcal·mol^{-1}) and the native ligand (–5.9 kcal·mol^{-1}). It should be noted that complexes ***IIIa*** and ***IIIb*** interact more effectively (–8.3, –8.1 kcal·mol^{-1}, respectively) with the alpha2 nicotinic acetylcholine receptor (PDB ID:**5FJV**) compared to complexes ***IIIc*** and ***IIId*** (–6.9 and –6.6 kcal·mol^{-1}, respectively), which may be due to a larger number of intermolecular interactions (Table 7).

Table 7

Protein 5FJV — Ligand intermolecular interactions

Ligand	Conventional Hydrogen Bond	Carbon Hydrogen Bond	Pi-Pi T-shaped	Pi-Donor	Pi-Sigma	Pi-Sulfur	Pi-alkyl	Pi-Pi-Stacked
IIIa	TRP115	ARG49, ALA48	TRP178	THR179	VAL120	MET134	ALA130	–
IIIb	–	–	TRP178	THR179	ALA130, VAL120	MET134	–	–
IIIc	–	–	–	–	–	–	VAL120, ALA130	PHE129, TRP178
IIId	ARG49	–	–	ALA48	MET134, ALA48	–	–	–
Reference Drug								
Bupropion	GLU128, THR132	–	–	–	–	–	ILE152, TYR153, HIS133, ALA151	–
Native ligand	TYR122, TRP178	–	–	–	–	–	CYS221, CYS222, TYR219, TYR226	–

As can be seen in Table 7, ligand ***IIIa*** forms 8 bonds with amino acids of the target protein **5FJV**, including one Conventional Hydrogen Bond with TRP115, two Carbon Hydrogen Bond with ARG49, ALA48, one Pi-Pi T-shaped with TRP178, Pi-Donor with THR179, Pi-Sigma with VAL120, Pi-Sulfur with MET134, Pi-alkyl with ALA130. Ligand ***IIIb*** forms 5 bonds with amino acids of the target protein 5FJV, including one Pi-Pi T-shaped with TRP178, one Pi-Donor with THR179, two Pi-Sigma with ALA130 and VAL120, one Pi-Sulfur with MET134. Ligand ***IIIc*** forms four bonds with amino acids of the target protein 5FJV, including two Pi-alkyl with VAL120 and ALA130, two Pi-Pi-Stacked with PHE129 and TRP178. Ligand ***IIId*** forms 4 bonds with amino acids of the target protein 5FJV, including one Conventional Hydrogen Bond with ARG49, one Pi-Donor with ALA48, two Pi-Sigma with MET134 and ALA48 (Figures 6, S2-S5).

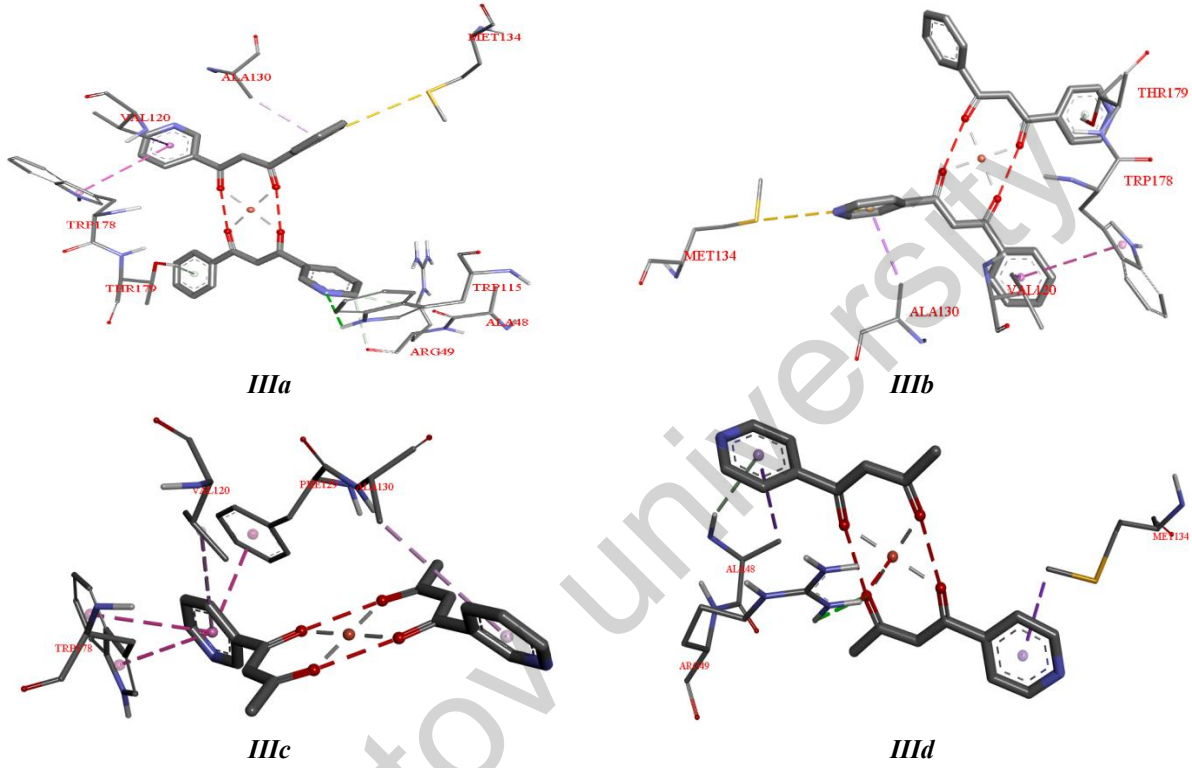

Figure 6 Visualization of protein **5FJV** amino acids — ligand ***IIIa-d*** interactions

As can be seen in Figures 6, S2-S5, the pi-electron systems of the pyridyl and benzene rings of the studied ligands ***IIIa-d*** actively participate in intermolecular interactions, therefore their greater number in ligands ***IIIa*** and ***IIIb*** leads to a more effective interaction of these compounds with the target protein **5FJV**.

Overall, molecular docking simulations of synthesized copper complexes ***IIIa-d*** with alpha2 nicotinic acetylcholine receptor (PDB ID:**5FJV**) showed their high potential as nicotinic receptor antagonist. Moreover, compounds ***IIIa*** and ***IIIb*** showed a more effective interaction with the **5FJV** protein compared to compounds ***IIIc*** and ***IIId***, may be due to the presence of a larger number of substituents with pi-electron systems.

Conclusions

We have obtained previously unknown chelate complexes of copper(II) with pyridyl-containing beta-diketonates. The syntheses were carried out with different ratios of reagents, the most successful was the ratio of 2:1 1,3-diketone to copper(II) acetate. Complexation with copper(II) took place at a temperature not exceeding 50 ºC for 1 hour, with the yield of products ***IIIa–d*** ranging from 8.5 % to 31.3 %. The structure of the newly obtained chelates has been proven by IR, atomic emission spectroscopy and mass spectrometry. Based on DFT B3LYP/6-311++G(d, p) /LanL2DZ CPCM (water) calculations, the non-planar structure of the synthesized copper chelate complexes ***IIIa-d*** was demonstrated, an analysis of the HOMO-LUMO orbitals and molecular electrostatic potential (MEP) was performed, global descriptors of chemical activity were assessed. *In silico* study of biological activity was carried out using the PASS Prediction and AutoDock Vina tools. Molecular docking simulations of synthesized copper complexes ***IIIa-d*** with alpha2 nicotinic acetylcholine receptor (PDB ID:**5FJV**) showed their high potential as nicotinic receptor antagonist. Moreover,

compounds ***IIIa*** and ***IIIb*** showed a more effective interaction with the **5FJV** protein compared to compounds ***IIIc*** and ***IIId***, may be due to the presence of a larger number of substituents with pi-electron systems. Newly synthesized copper complexes ***IIIa*** and ***IIIb*** can be recommended for further study of their pharmaceutical potential as nicotinic receptor antagonist via *in vitro* and *in vivo* methods.

Supporting Information

The Supporting Information is available free at https://ejc.buketov.edu.kz/index.php/ejc/article/view/124/211

Funding

Authors state no funding involved.

*Author Information**

**The authors' names are presented in the following order: First Name, Middle Name and Last Name*

Alexey Aleksandrovich Kukushkin (*corresponding author*) — PhD, Associate Professor, School of Petroleum and Gas Engineering, Siberian Federal University, pr. Svobodny, 79, 660041, Krasnoyarsk, Russia; e-mail: alekseykukushkin@bk.ru, https://orcid.org/0000-0002-2039-5471

Elizaveta Vitalievna Kudashova — Student, Department of Organic Chemistry and Technology of Organic Compounds, Reshetnev Siberian State University of Science and Technology, Krasnoyarskiy Rabochiy Ave., 31, 660037, Krasnoyarsk, Russia; e-mail: kudasovaelizaveta@gmail.com

Evgeny Vladimirovich Root — PhD, Head of the Department of Organic Chemistry and Technology of Organic Compounds, Reshetnev Siberian State University of Science and Technology, Krasnoyarskiy Rabochy Ave., 31, 660037, Krasnoyarsk, Russia; Associate Professor of the Department of Pharmacy with PC, State Medical University named after Prof. V.F. Voino-Yasenetsky, Partizana Zheleznyaka str., 1, 660022, Krasnoyarsk, Russia; e-mail: rootev@mail.ru, https://orcid.org/0009-0001-7093-4701

Anna Sergeevna Kositsyna — PhD, Associate Professor, Department of Organic Chemistry and Technology of Organic Compounds, Reshetnev Siberian State University of Science and Technology, Krasnoyarskiy Rabochiy Ave., 31, 660037, Krasnoyarsk, Russia; e-mail: kositsyna-anna@mail.ru

Ilya Sergeyevich Ponomarev — Junior Research Assistant, Institute of Chemistry and Chemical Technology Siberian Branch of the Russian Academy of Sciences, Akademgorodok str., 50/24, 660036, Krasnoyarsk, Russia, e-mail: il.p0nomarew@yandex.ru, https://orcid.org/0000-0001-7027-7177

Alexey Viktorovich Lyubyashkin — Director of the Institute of Chemical Technology, Reshetnev Siberian State University of Science and Technology, Krasnoyarskiy Rabochiy Ave., 31, 660037, Krasnoyarsk, Russia; e-mail: lyubyashkinav@sibsau.ru, https://orcid.org/0000-0002-0428-5950

Irina Anatolievna Pustolaikina — Candidate of Chemical Sciences, Associate Professor, Department of Physical and Analytical Chemistry, Karaganda Buketov University, Universitetskaya street, 28, 100024, Karaganda, Kazakhstan; e-mail: pustolaikina_irina@buketov.edu.kz, https://orcid.org/0000-0001-6319-666X

Author Contributions

The manuscript was written through contributions of all authors. All authors have given approval to the final version of the manuscript. CRediT: **Alexey Aleksandrovich Kukushkin** — investigation, methodology, validation; **Elizaveta Vitalievna Kudashova —** conceptualization, data curation, **Evgeny Vladimirovich Root** — data curation, formal analysis, visualization; **Anna Sergeevna Kositsyna —** validation, writing-original draft; **Ilya Sergeyevich Ponomarev —** investigation, methodology**; Alexey Viktorovich Lyubyashkin** — funding acquisition, resources; **Irina Anatolevna Pustolaikina —** computational study, methodology, investigation, data curation, formal analysis, visualization; writing-review & editing.

Acknowledgments

The work was carried out using the equipment of the Krasnoyarsk Regional Center for Collective Use of the Federal Research Center of the KSC SB RAS.

Conflicts of Interest

The authors declare no conflict of interest.

References

1 Harwood, J. (1963). *Industrial applications of organometallic compounds*. Chapman&Hall.

2 Rykowska I., & Wasiak W. (2002). Gas chromatography silica packings with chemically bonded complexes of Cu (II) and Cr (III). *Analytica Chimica*, 2, 271–278. https://doi.org/10.1016/S0003-2670(01)01404-0

3 Patel R.N. et al. (2009). Copper (II) complexes as superoxide dismutase mimics: synthesis, characterization, crystal structure and bioactivity of copper (II) complexes. *Inorganica Chimica, 14*, 4891–4898. https://doi.org/10.1016/j.ica.2009.07.037

4 Kalarani R. et al. (2020). Synthesis, spectral, DFT calculation, sensor, antimicrobial and DNA binding studies of Co (II), Cu (II) and Zn (II) metal complexes with 2-amino benzimidazole Schiff base. *Journal of Molecular Structure, 1206,* 127725. https://doi.org/10.1016/j.molstruc.2020.127725

5 Mir, I.A., Ain, Q.U., Singh, I., Carmieli, R., & Sharma, R. (2024). Investigation of biological activity of oxindole semicarbazones based copper (II) complexes: Synthesis, antimicrobial activities and molecular modelling. *Polyhedron, 263*, 117208. https://doi.org/10.1016/j.poly.2024.117208

6 Hassan, S.S., Aly, S.A., Rizk, N.M.H., Khidr, M.A., Al-Sulami, A.I., Mousa, I.E., Badr, E.E., & Abdalla, E.M. (2024). Synthesis, characterization, antimicrobial, anticancer and the theoretical calculation of a novel N,O-multidentate chelating ligand and its Cu(II) and Fe(III) complexes. *Inorganic Chemistry Communications, 170*, 113279. https://doi.org/10.1016/j.inoche.2024.113279

7 Karcz D. et al. (2021). Novel coumarin-thiadiazole hybrids and their Cu (II) and Zn (II) complexes as potential antimicrobial agents and acetylcholinesterase inhibitors. *International Journal of Molecular Sciences, 22*(18), 9709. https://doi.org/10.3390/ijms22189709

8 Stepanenko I. et al. (2021). Coumarin-Based Triapine Derivatives and Their Copper (II) Complexes: Synthesis, Cytotoxicity and mR2 RNR Inhibition Activity. *Biomolecules, 11*(6), 862. https://doi.org/10.3390/biom11060862.

9 Dey, S.K., Bag, B., Zhou, Z., Chan, A.S., & Mitra, S. (2004). Synthesis, characterization and crystal structure of a monomeric and a macrocyclic copper (II) complex with a large cavity using benzylacetylacetone ligand. *Inorganica chimica acta, 357*(7), 1991–1996. https://doi.org/10.1016/j.ica.2003.12.014.

10 Pauly, M.A., Erwin, E.M., Powell, D.R., Rowe, G.T., & Yang, L. (2015). A synthetic, spectroscopic and computational study of copper (II) complexes supported by pyridylamide ligands. *Polyhedron*, 102, 722–734. https://doi.org/10.1016/j.poly.2015.11.015.

11 Walczak, A., Kurpik, G., & Stefankiewicz, A.R. (2020). Intrinsic effect of pyridine-n-position on structural properties of Cu-based low-dimensional coordination frameworks. *International Journal of Molecular Sciences, 21*(17), 6171. https://doi.org/10.3390/ijms21176171.

12 Dudek, M. et al. (2011). Interaction of Copper (II) with Ditopic Pyridyl-β-diketone Ligands: Dimeric, framework, and metallogel structures. *Crystal growth & design, 11*(5), 1697–1704. https://doi.org/10.1021/cg101629w.

13 Bendi, A., Jafar Ahamed, A., Kaur, N., Mujafarkani, N., Banu, A.M., & Afshari, M. (2025). Synthesis, Experimental and Computational Evaluation of p-Semidine-p-Phenylenediamine-Formaldehyde (Terpolymer) and Its Copper Complex as Potent Antimicrobial and Anticorrosive Agents. *Journal of Inorganic and Organometallic Polymers and Materials, 35,* 3993–4015. https://doi.org/10.1007/s10904-024-03507-4

14 Quim Peña et al. (2021). Copper(II) N,N,O-Chelating Complexes as Potential Anticancer Agents. *Inorg. Chem., 60, 5*, 2939–2952. https://doi.org/10.1021/acs.inorgchem.0c02932.

15 Gur'eva, Ya.A., Zalevskaya, O.A., & Kuchin, A.V. (2023). Biologically Active Palladium(II), Zinc(II), and Copper(II) Complexes with Terpene Ligands as Potential Pharmaceutical Drugs. *Russian Journal of Coordination Chemistry, 49*(10), 631–651. https://doi.org/10.1134/s1070328423700665

16 Carlos Martínez-Ceberio et al. (2023). Mesomorphism and luminescence in coordination compounds and ionic salts based on pyridine-functionalized β-diketones. Influence of the pyridine nitrogen position. *Journal of Molecular Liquids, 385*, 1, 122290. https://doi.org/10.1016/j.molliq.2023.122290.

17 de Gonzalo, G., & Alcántara, A.R. (2021). Recent Developments in the Synthesis of β-Diketones. *Pharmaceuticals, 14*(10), 1043. https://doi.org/10.3390/ph14101043

18 Kljun, J., & Turel, I. (2017). β-Diketones as Scaffolds for Anticancer Drug Design — From Organic Building Blocks to Natural Products and Metallodrug Components. *European Journal of Inorganic Chemistry, 2017*(12), 1655–1666. Portico. https://doi.org/10.1002/ejic.201601314

19 Famta, P., et al. (2025). Hydroxypropyl β-cyclodextrin complexes of olaparib: Amalgamation of *in silico*, *in vitro* and *in vivo* approaches for bioavailability enhancement. *Journal of Molecular Structure, 1336*, 142077. https://doi.org/10.1016/j.molstruc.2025.142077

20 Iqtadar, R., et al. (2025). New halogenated chalcones as potential anti-inflammatory agents: A comprehensive *in silico*, *in vitro*, and *in vivo* study with ADME profiling. *Journal of Molecular Structure, 1326*, 141055. https://doi.org/10.1016/j.molstruc.2024.141055.

21 Rakhimzhanova, A.S., Muzaparov, R.A., Pustolaikina, I.A., Kurmanova, A.F., Nikolskiy, S.N., Kapishnikova, D.D., Stalinskaya, A.L., & Kulakov, I.V. (2024). Series of Novel Integrastatins Analogues: In silico Study of Physicochemical and Bioactivity Parameters. *Eurasian Journal of Chemistry, 29*(4 (116)), 44–60. https://doi.org/10.31489/2959-0663/4-24-13

22 Interstate standard (1980). Technical ethyl alcohol. Specifications (GOST 17299-78). https://docs.cntd.ru/document/120.

23 Levine R., & Sneed J.K. (1951). The relative reactivities of the isomeric methyl pyridinecarboxylates in the acylation of certain ketones. The synthesis of β-diketones containing pyridine rings. *Journal of the American Chemical Society, 73*(12), 5614–5616. https://doi.org/10.1021/ja01156a035.

24 Rusnac, R., Garbuz, O., Chumakov, Y., Tsapkov, V., Hureau, C., Istrati, D., & Gulea, A. (2023). Synthesis, Characterization, and Biological Properties of the Copper(II) Complexes with Novel Ligand: N-[4-({2-[1-(pyridin-2-yl)ethylidene]hydrazinecarbothioyl}amino)phenyl]acetamide. *Inorganics, 11*(10), 408. https://doi.org/10.3390/inorganics11100408

25 Kulakov, I.V., Stalinskaya, A.L., Chikunov, S.Y., Pustolaikina, I.A., & Gatilov, Y.V. (2023). Synthesis of New Structural Analogues of Natural Integrastatins with a Basic Epoxybenzo[7,8]oxocine Skeleton: Combined Experimental and Computational Study. *Synthesis, 56*(02), 329–345. CLOCKSS. https://doi.org/10.1055/s-0042-1751521

26 Stalinskaya, A.L., Chikunov, S.Y., Pustolaikina, I.A., & Kulakov, I.V. (2022). Cyclization Reaction of 3,5-Diacetyl-2,6-dimethylpyridine with Salicylic Aldehyde and Its Derivatives: Quantum-Chemical Study and Molecular Docking. *Russian Journal of General Chemistry, 92*(5), 914–924. https://doi.org/10.1134/s107036322205022x

27 Alghuwainem, Y.A.A., El-Lateef, H.M.A., Khalaf, M.M., Amer, A.A., Abdelhamid, A.A., Alzharani, A.A., Alfarsi, A., Shaaban, S., Gouda, M., & Abdou, A. (2022). Synthesis, DFT, Biological and Molecular Docking Analysis of Novel Manganese(II), Iron(III), Cobalt(II), Nickel(II), and Copper(II) Chelate Complexes Ligated by 1-(4-Nitrophenylazo)-2-naphthol. *International Journal of Molecular Sciences, 23*(24), 15614. https://doi.org/10.3390/ijms232415614

28 Gaussian 16, Revision A.03, M.J. Frisch, G.W. Trucks, H.B. Schlegel, G.E. Scuseria, M.A. Robb, J.R. Cheeseman, G. Scalmani, V. Barone, G.A. Petersson, H. Nakatsuji, X. Li, M. Caricato, A.V. Marenich, J. Bloino, B.G. Janesko, R. Gomperts, B. Mennucci, H.P. Hratchian, J.V. Ortiz, A.F. Izmaylov, J.L. Sonnenberg, D. Williams-Young, F. Ding, F. Lipparini, F. Egidi, J. Goings, B. Peng, A. Petrone, T. Henderson, D. Ranasinghe, V.G. Zakrzewski, J. Gao, N. Rega, G. Zheng, W. Liang, M. Hada, M. Ehara, K. Toyota, R. Fukuda, J. Hasegawa, M. Ishida, T. Nakajima, Y. Honda, O. Kitao, H. Nakai, T. Vreven, K. Throssell, J.A. Montgomery, Jr., J.E. Peralta, F. Ogliaro, M.J. Bearpark, J.J. Heyd, E.N. Brothers, K.N. Kudin, V.N. Staroverov, T.A. Keith, R. Kobayashi, J. Normand, K. Raghavachari, A.P. Rendell, J.C. Burant, S.S. Iyengar, J. Tomasi, M. Cossi, J.M. Millam, M. Klene, C. Adamo, R. Cammi, J.W. Ochterski, R.L. Martin, K. Morokuma, O. Farkas, J.B. Foresman, and D.J. Fox, Gaussian, Inc., Wallingford CT, 2016.

29 Tomasi, J., Mennucci, B., & Cammi, R. (2005). Quantum mechanical continuum solvation models. *Chemical Reviews, 105*(8), 2999–3094. https://doi.org/10.1021/cr9904009

30 Molski, M. (2021). Theoretical modeling of structure-toxicity relationship of cyanides. *Toxicology Letters, 349*, 30–39. https://doi.org/10.1016/j.toxlet.2021.05.011

31 Dennington, R., Keith, T., & Millam, J. GaussView, Version 6. Semichem Inc., Shawnee Mission, KS, 2016. http://gaussian.com

32 Poroikov, V.V., Filimonov, D.A., Gloriozova, T.A., Lagunin, A.A., Druzhilovskiy, D.S., Rudik, A.V., Stolbov, L.A., Dmitriev, A.V., Tarasova, O.A., Ivanov, S.M., & Pogodin, P.V. (2019). Computer-aided prediction of biological activity spectra for organic compounds: the possibilities and limitations. *Russian Chemical Bulletin, 68*(12), 2143–2154. https://doi.org/10.1007/s11172-019-2683-0

33 Filimonov, D.A., Lagunin, A.A., Gloriozova, T.A., Rudik, A.V., Druzhilovskii, D.S., Pogodin, P.V., & Poroikov, V.V. (2014). Prediction of the Biological Activity Spectra of Organic Compounds Using the Pass Online Web Resource. *Chemistry of Heterocyclic Compounds, 50*(3), 444–457. https://doi.org/10.1007/s10593-014-1496-1

34 Filimonov, D.A., Rudik, A.V., Dmitriev, A.V., & Poroikov, V.V. (2020). Computer-Aided Estimation of Biological Activity Profiles of Drug-Like Compounds Taking into Account Their Metabolism in Human Body. *International Journal of Molecular Sciences, 21*(20), 7492. https://doi.org/10.3390/ijms21207492

35 Sarkar, A., Concilio, S., Sessa, L., Marrafino, F., & Piotto, S. (2024). Advancements and novel approaches in modified Autodock Vina algorithms for enhanced molecular docking. *Results in Chemistry*, 101319. https://doi.org/10.1016/j.rechem.2024.101319

36 Forli, S., Huey, R., Pique, M.E., Sanner, M.F., Goodsell, D.S., & Olson, A.J. (2016). Computational protein–ligand docking and virtual drug screening with the AutoDock suite. *Nature Protocols, 11*(5), 905–919. https://doi.org/10.1038/nprot.2016.051

37 BIOVIA. (2023). BIOVIA Discovery Studio. Dassault Systèmes.

38 Kostyuk, N.N., & Dick, T.A. (2020). Synthesis of Ultrapure Copper Chelates. *Russian Journal of General Chemistry, 90*(11), 2141–2146. https://doi.org/10.1134/s1070363220110195.

39 Rollema, H., Bertrand, D., & Hurst, R.S. (2010). Nicotinic Agonists and Antagonists. In: Stolerman, I.P. (Eds). *Encyclopedia of Psychopharmacology*. Springer, Berlin, Heidelberg. https://doi.org/10.1007/978-3-540-68706-1_304

40 Crooks, P.A., Bardo, M.T., & Dwoskin, L.P. (2014). Nicotinic Receptor Antagonists as Treatments for Nicotine Abuse. *Emerging Targets & Therapeutics in the Treatment of Psychostimulant Abuse*, 513–551. https://doi.org/10.1016/b978-0-12-420118-7.00013-5

41 Wu, C.-H., Lee, C.-H., & Ho, Y.-S. (2011). Nicotinic Acetylcholine Receptor-Based Blockade: Applications of Molecular Targets for Cancer Therapy. *Clinical Cancer Research, 17*(11), 3533–3541. https://doi.org/10.1158/1078-0432.ccr-10-2434

42 Kouvatsos, N., Giastas, P., Chroni-Tzartou, D., Poulopoulou, C., & Tzartos, S. J. (2016). Crystal structure of a human neuronal nAChR extracellular domain in pentameric assembly: Ligand-bound α2 homopentamer. *Proceedings of the National Academy of Sciences,* 113(34), 9635–9640. https://doi.org/10.1073/pnas.1602619113

43 Giastas, P., Kouvatsos, N., Chroni-Tzartou, D., & Tzartos, S.J. (2016). *Crystal structure of the extracellular domain of alpha2 nicotinic acetylcholine receptor in pentameric assembly*. https://doi.org/10.2210/pdb5fjv/pdb

44 (2025). National Center for Biotechnology Information. PubChem Compound Summary for CID 444, Bupropion. Retrieved from https://pubchem.ncbi.nlm.nih.gov/compound/Bupropion